Journal of Hazardous Materials 299 (2015) 361–370

Contents lists available at ScienceDirect

Journal of Hazardous Materials

journal homepage: www.elsevier.com/locate/jhazmat

Proteomic analysis of cell proliferation in a human hepatic cell line (HL-7702) induced by perfluorooctane sulfonate using iTRAQ

Ruina Cui[a,1], Hongxia Zhang[a,1], Xuejiang Guo[b], Qianqian Cui[a], Jianshe Wang[a], Jiayin Dai[a,*]

[a] Key Laboratory of Animal Ecology and Conservation Biology, Institute of Zoology, Chinese Academy of Sciences, Beijing 100101, PR China
[b] State Key Laboratory of Reproductive Medicine, Department of Histology and Embryology, Nanjing Medical University, Nanjing 210029, PR China

HIGHLIGHTS

- PFOS stimulates cell proliferation of human liver cell line (HL-7702).
- Differential expressed proteins are identified by iTRAQ.
- Most of differential proteins caused by PFOS are related to cell proliferation.
- Up-regulation of cyclin/cdk by PFOS plays a role in driving cells into cell cycle.

ARTICLE INFO

Article history:
Received 8 May 2015
Received in revised form 8 June 2015
Accepted 18 June 2015
Available online 23 June 2015

Keywords:
PFOS
iTRAQ
Cell proliferation
Cell cycle
Cyclins

ABSTRACT

Perfluorooctane sulfonate (PFOS) is a commonly used and widely distributed perfluorinated compound proven to cause adverse health outcomes. However, how PFOS affects liver cell proliferation is not well understood. In this experiment, we exposed a human liver cell line (HL-7702) to 50 μM PFOS for 48 h and 96 h. We identified 52 differentially expressed proteins using a quantitative proteomic approach. Among them, 27 were associated with cell proliferation, including hepatoma-derived growth factor (Hdgf) and proliferation biomarkers Mk167 (Ki67) and Top2α. Results from MTT, cell counting, and cell cycle analysis showed low-dose PFOS (<200 μM) stimulated HL-7702 cell viability at 48 h and 96 h, reduced the G0/G1 percentage, and increased the S + G2/M percentage. Moreover, levels of Cyclin D1, Cyclin E2, Cyclin A2, Cyclin B1 and their partner Cdks were elevated, and the expression of regulating proteins like c-Myc, p53, p21 waf/cip1 and Myt1, as well as the phosphorylation levels of p-Wee1(S642), p-Chk1(S345) and p-Chk2(T68), were disturbed. We hypothesized that low-dose PFOS stimulated HL-7702 proliferation by driving cells into G1 through elevating cyclins/cdks expression, and by promoting cell cycle progression through altering other regulating proteins. This research will shed light on the mechanisms behind PFOS-mediated human hepatotoxicity.

1. Introduction

Perfluoroalkyl acids (PFAAs) are a large group of man-made compounds with strong carbon-fluorine bonds that are stable to metabolic and environmental degradation. Perfluorooctane sulfonate (PFOS) is a widely used PFAA in commercial and industrial applications such as surfactants, lubricants, paints, polishes, paper and textile coatings, food packaging and fire-retardant foams [1]. Due to its persistence and widespread use, PFOS has been found in air, water, sediment, animals and humans [2–6]. Humans are likely exposed to PFOS via oral, inhalation and dermal routes, with the liver and blood, the main organs in which is PFOS distributed, although it has also been identified in umbilical cord blood, amniotic fluid and breast milk [7–9]. Studies on an occupational population retired from a 3 M plant where PFOS was produced showed decreased PFOS serum concentrations from 145-3,490 ng/mL to 37-1,740 ng/mL during a five year period, indicating that the mean serum elimination half-life of PFOS was 5.4 years [10]. Epidemiological studies also showed correlations between

Abbreviations: MTT, 3-(4,5-dimethylthiazol-2-yl)-2,5-diphenyltetrazolium bromide; iTRAQ, isobaric tags for relative and absolute quantitation; Cdks, cyclin-dependent kinases; Myc, myelocytomatosis oncogene; Myt1, myelin transcription factor 1; Wee1, G2 checkpoint kinase, M phase inhibitor protein kinase; p21 waf/cip1, cyclin-dependent kinase inhibitor 1A; Chk, Checkpoint kinase.

* Corresponding author at: Key Laboratory of Animal Ecology and Conservation Biology, Institute of Zoology, Chinese Academy of Sciences, Beijing 100101, PR China. Fax: +86 10 64807099.
E-mail address: daijy@ioz.ac.cn (J. Dai).

[1] Ruina Cui and Hongxia Zhang contributed equally to this paper.

http://dx.doi.org/10.1016/j.jhazmat.2015.06.031
0304-3894/

elevated PFOS serum levels and liver function damage [11–13], hypertension risk (high uric acid) [14] and reduced sperm quality [15].

Studies on PFOS-elicited hepatotoxicity in rodent models and *in vitro* systems further revealed that PFOS tended to accumulate in the liver and disrupted the expression of genes involved in carbohydrate, fatty acid and energy metabolism [16,17]. PFOS also reportedly induced hepatomegaly and hepatocellular hypertrophy, hepatic steatosis and hepatic adenomas in rodents due to the activation of peroxisome proliferator-activated receptors (PPARs) [18,19]. PFOS and other PFAAs were demonstrated as agonists of PPAR, and a species difference was observed *in vitro*, showing that human PPAR was less responsive than murine PPAR across various PFAAs [20,21]. This difference suggests a limitation in species extrapolation in the health risk assessment of PFAAs. Therefore, the mechanism of PFOS-induced human hepatotoxicity remains unclear and still needs further investigation.

The use of proteomics in toxicological studies, in which global protein information is provided, can elucidate the molecular mechanisms underlying pollutant toxicity [22]. Isobaric tags for relative and absolute quantitation (iTRAQ) is one of the most widely used proteomic approaches, and can exhibit a large dynamic range in profiling proteins at either high or low abundance and can simultaneously identify and quantify differentially expressed proteins among four to eight different specimens, thus increasing throughput while reducing experimental error.

In the present study, a non-tumor fetal human liver cell line (HL-7702) was chosen as the *in vitro* system to illuminate the effect of PFOS on human hepatotoxicity. We identified differentially expressed proteins in HL-7702 after PFOS exposure for 48 h and 96 h using iTRAQ coupled with liquid chromatography electrospray ionization tandem mass spectrometry (LC-ESI–MS/MS). The differential expressions of some important proteins were further validated by western blot analysis. According to bioinformatics analysis of the interaction relationships among the proteins identified above, MTT, cell counting, and cell cycle analysis were used to investigate the effects of PFOS on hepatocellular proliferation. This research will help provide novel insight into the molecular mechanisms involved in human hepatotoxicity of PFOS.

2. Materials and methods

2.1. Chemicals

Perfluorooctane sulfonate (PFOS) (potassium salt, purity >98%) (CAS number 2795-39-3) was purchased from Sigma–Aldrich (MO, USA). The RPMI-1640 complete culture medium and trypsin solution (0.25%) were purchased from Hyclone (UT, USA), and fetal bovine serum was obtained from Lanzhou Bailing Biotechnology Co., Ltd. (Lanzhou, China). RIPA lysis buffer was obtained from Thermo Fisher (USA). The BCA kit and enhanced chemiluminescence solution (superECL) were purchased from Tiangen Biotech Co., Ltd. (Beijing, China). The iTRAQ analysis kit was obtained from ABI (Foster City, USA). Cell cycle and apoptosis analysis kits and primary antibodies (β-Actin, β-Tubulin, Gapdh) were purchased from Beyotime Biotechnology (Shanghai, China). The primary antibodies against Cps1 (ab129076) and MK167 (Ki67) (ab15580) were purchased from Abcam (Hong Kong). Antibodies against Hdgf (11344-1-AP) and c-Myc (10057-1-AP) were purchased from Proteintech (Chicago, USA). Other primary antibodies used for detecting Ncl (CST#12247), Top2α (CST#4733), Cyclin D1 (CST#2978), Cyclin E2 (CST#4132), Cyclin A2 (CST#4656), Cyclin B1 (CST#12231), CDK6 (CST#3136), p53 (CST#2524), p-Chk1 (S345) (CST#2348), p-Chk2 (T68) (CST#2197), p-Cdc2 (Y15) (CST#4539), p-wee1 (S642) (CST#4910), Myt1 (CST#4282), and p21 waf1/Cip1 (CST#2947) were purchased from Cell Signaling Technology, Inc (USA). The secondary IgG-HRP antibodies were purchased from Santa Cruz Biotechnology (USA). Dimethyl sulfoxide (DMSO), MTT and all other chemicals were of analytical or biochemical grade and were purchased from Sigma–Aldrich (MO, USA).

2.2. Cell culture and treatment

The HL-7702 cell line was purchased from the Shanghai Institute of Cell Biology, Chinese Academy of Sciences. Cells were cultured in RPMI-1640 complete culture medium containing 10% fetal bovine serum in an incubator at 37 °C, supplied with 5% CO_2. PFOS was dissolved in DMSO for the stock solution and the final concentration of DMSO in all working solutions was 0.1% to ensure it did not induce cell cytotoxicity. For MTT assay, HL-7702 cells were trypsinized and seeded in 96-well plates at initial densities of 1×10^4 cells/well and 3×10^3 cells/well for 48 h and 96 h exposure, respectively. For cell counting, cell cycle analysis and protein extraction, cells were seeded in 6-well plates at initial densities of 2×10^5 cells/well and 8×10^4 cells/well for 48 h and 96 h exposure, respectively. The cells were allowed to attach for 24 h before treatment.

2.3. MTT assay, cell counting and protein extraction

The MTT working solution (5 mg/mL) was filtered with a MILLEX® GP filter unit (0.22 μm) (Merck Millipore, Billerica, MA, USA) to remove bacteria and then stored at 4 °C, avoiding light. After PFOS exposure for 48 h and 96 h at a range of concentrations, 20 μL of MTT was added to the medium in each well of the 96-well plates followed by incubation at 37 °C for 4 h. The supernatant was removed and then replaced by 150 μL of DMSO to dissolve the produced formazan. The absorbance (Abs) was measured using a microplate reader at 490 nm. The relative cell viability (%) related to the control wells containing cell culture media without PFOS was calculated by $[Abs]_{test}/[Abs]_{control} \times 100$.

The HL-7702 cells were seeded in 6-well plates and then treated by PFOS at 0 (DMSO), 50, 100 and 200 μM for 48 h and 96 h. After exposure, cells were trypsinized and suspended in PBS with equal volume (pH 7.4). We took 10 μL of cell suspension to calculate cell number using a Bio-Rad TC10 automated cell counter (Bio-Rad, Hercules, USA), and then centrifuged the suspension to gather cells for protein extraction. Proteins were extracted using RIPA lysis buffer containing a protease inhibitor (PMSF) and phosphatase inhibitor cocktail, and concentrations were measured using a BCA kit.

2.4. Protein preparation, iTRAQ labeling and strong cationic exchange (SCX) fractionation

Our previous study showed no inhibitory effect of PFOS on HL-7702 cell viability at 423 μM (IC_0) for 48 h [29]. Thus, to avoid cytotoxicity, 50 μM PFOS (≈1/10 IC_0) was chosen to investigate the differential expression of proteins caused by PFOS. HL-7702 cells were collected from the control group and 50 μM PFOS group treated for 48 h and 96 h, respectively. The cells obtained from each group were pooled as one mixed biological sample to represent that particular group. This exposure experiment was repeated and two replicates per group were obtained for iTRAQ analysis to identify differentially expressed proteins. Each sample was sonicated for 15 min in 500 μL of lysis buffer (2 M thiourea, 7 M urea, 4% 3-[(3-cholamidopropyl) dimethylammonio]propanesulfonate (CHAPS), 40 mM Tris-HCl, pH 8.5) containing 1 mM phenylmethanesulfonylfluoride (PMSF), 2 mM EDTA and 10 mM dithiothreitol (DTT), then centrifuged at 25,000 × g for 20 min at 4 °C. The proteins in the collected supernatant were reduced at 56 °C for 1 h in 10 mM DTT, then alkylated in the dark with 55 mM iodoacetamide (IAM) for 45 min, and subsequently precipitated using acetone at −20 °C.

The protein precipitates were dissolved in 200 μL of 0.5 M triethylammonium bicarbonate (TEAB) by sonication for 15 min. Protein concentration was measured using the Bradford assay.

A 100 μg portion of protein from each extract was digested with trypsin at 37 °C for 12 h. Subsequently, the tryptic peptides in eight mixed samples of four groups (two mixed samples per group) were labeled with iTRAQ reagents (ABI, Foster City, USA) (isobaric tags 115 and 114 for the control and PFOS-exposed group treated for 48 h, respectively, and 119 and 118 for the control and PFOS-exposed group treated for 96 h, respectively).

The labeled peptides were pooled together, dried by vacuum centrifugation and reconstituted in 4 mL buffer A (25 mM NaH_2PO_4 in 25% ACN, pH 2.7), and then fractionated by SCX chromatography using a Shimadzu LC-20AB HPLC pump system (Shimadzu, Japan) linked to a 4.6 mm × 250 mm Ultremex SCX column (Phenomenex, USA) with a 1 mL/min flow rate. The mobile phase consisted of buffer A (25 mM NaH_2PO_4 in 25% ACN, pH 2.7) and buffer B (25 mM NaH_2PO_4, 1 M KCl in 25% ACN, pH 2.7). The following linear gradient was used: buffer A for 10 min, 5–35% buffer B for 11 min and then 35–80% buffer B for 1 min. Elution was monitored by measuring the absorbance at 214 nm and fractions were collected every 1 min. The eluted peptides were combined into 12 fractions, desalted with a Strata X C18 column (Phenomenex, USA) and lyophilized.

2.5. LC-ESI–MS/MS analysis

Mass spectroscopic (MS) analysis was performed with a Triple TOF 5600 mass spectrometer (AB SCIEX, Concord, ON, Canada) coupled with a nanoACQuity HPLC system (Waters, USA). Microfluidic traps and nanofluidic columns packed with Symmetry C18 (5 μm, 180 μm × 20 mm) were employed in online trapping and desalting, and nanofluidic columns packed with BEH130C18 (1.7 μm, 100 μm × 100 mm) were utilized for analytical separation. The mobile phases were composed of water/acetonitrile/formic acid (A: 98/2/0.1%; B: 2/98/0.1%) and calibration liquid (Thermo Fisher Scientific, USA). A 2.25 μg (9 μL) portion of the sample was loaded, trapped and desalted with buffer A at a flow rate of 2 μL/min for 15 min, then separated using the following gradient at a flow rate of 300 nL/min: 5% buffer B for 1 min, 5–35% buffer B for 40 min, 35–80% buffer B for 5 min, and 80% buffer B for 5 min. Initial chromatographic conditions were restored after 2 min.

Data acquisition was carried out on a Triple TOF 5600 System (AB SCIEX, USA) fitted with a Nanospray III source (AB SCIEX, USA) using the following parameter settings: spray voltage, 2.5 kV; sheath gas (nitrogen) pressure, 35 psi; collision gas (argon) pressure, 15 psi; vaporizer temperature, 150 °C. Survey scans were acquired in 250 ms, and up to 30 product ion scans were collected if they exceeded a threshold of 120 counts per second (counts/s) with a 2+ to 5+ charge-state. A sweeping collision energy setting of 35 ± 5 eV coupled with iTRAQ adjusted rolling collision energy was applied to all precursor ions for collision-induced dissociation. Dynamic exclusion was set for half of the peak width (18 s), and the precursor was then refreshed off the exclusion list.

2.6. Database search and quantification

The acquired peak-lists of all MS/MS spectra were combined into one Mascot generic format (MGF) file and searched with Mascot software (version 2.3.02; Matrix Science, London, U.K.) against the International Protein Index (IPI) human sequence database (version 3.76, 89,378 sequences). Search parameters included the following: trypsin as the enzyme, with one missed cleavage allowed; fixed modifications of carbamidomethylation (Cys), iTRAQ 8-plex (N-term) and iTRAQ 8-plex (Lys); variable modifications of Gln- > pyro-Glu (N-term Gln), oxidation (Met) and iTRAQ 8-plex (Tyr); mass tolerance of 0.05 Da for peptides and 0.1 Da for fragmentations.

The search results were passed through additional filters before exporting the data. For protein identification, the filters were set as follows: a 95% confidence interval ($P < 0.05$) and expected cut-off or ion score of less than 0.05 (with 95% confidence). Protein quantification settings included the following: "median" protein ratio type; "summed intensities" normalization, and "automatic" outliers removal. Minimum precursor charge was set to 1, and minimum peptides were set to 2; only unique peptides were used to quantify proteins. The peptide threshold was set as above for the identity threshold.

The proteins up-regulated or down-regulated in both replicates with a relative quantification *P*-value both below 0.05 were regarded as being differentially expressed in the data.

Gene Ontology (GO) annotation of the identified proteins was done by searching the GO Web site (http://www.geneontology.org). To better understand these differentially expressed proteins in relation to published literature, interactions among these proteins regarding biological pathways were determined using Pathway Studio software via the ResNet database (version 6.5, Ingenuity Systems, Inc.).

2.7. Flow cytometer analysis of cell cycle

After the HL-7702 cells were exposed to PFOS (0, 50, 100 and 200 μM) for 48 h and 96 h in 6-well plates, they were trypsinized and washed with phosphate buffer solution (PBS) (pH 7.4), then fixed in 70% ethanol at 4 °C for 24 h. The fixed cells were washed with PBS, filtrated through screen filters and stained by propidium iodide (PI) staining solution (containing ribonuclease A) (Beyotime Biotechnology, China) for 30 min, and subsequently analyzed on a flow cytometer (BD FACSCallbur, Becton Dickinson, USA). Cells in different cell cycle phases were presented as a percentage of the total number of cells counted.

2.8. Western blot analysis

Equal amounts of protein (30 μg per lane) from each sample were separated on SDS-PAGE gel and transferred onto a PVDF membrane (GE Healthcare, UK). Membranes were blocked with 5% (w/v) non-fat milk or BSA in TBST for 1 h prior to overnight incubation at 4 °C with the primary antibodies. Immunoblots were performed with horseradish peroxidase (HRP)-conjugated secondary antibodies (anti-mouse or anti-rabbit IgG), and visualized by enhanced chemiluminescence reagents on X-ray films. Densitometry signals were analyzed with Quantity One Software (v 4.6.3, Bio-Rad, USA) and data were normalized to expression levels of β-actin or β-tubulin. All western blot analyses were conducted in triplicate.

2.9. Statistical analysis

The MTT, cell number, total protein amount, cell cycle distribution and western blot analysis results were presented as means ± standard errors (SE) for each experimental group of at least three individual samples. Differences between the control and treatment groups were analyzed by one-way analysis of variance (ANOVA) followed by Duncan's multiple range tests using SPSS 17.0 software. Probabilities of $P < 0.05$ were considered statistically significant.

3. Results

3.1. iTRAQ analysis and bioinformatics analysis for differentially expressed proteins induced by PFOS

To characterize the expression changes of proteins related to PFOS exposure, iTRAQ quantitative proteomic technology was used

Table 1
Differentially expressed proteins identified by iTRAQ in HL-7702 after 50 μM PFOS exposure for 48 h and 96 h.

Number	Accession	Gene	Protein	Fold change (50 μM vs. Control)		Function description
	Number	Name	Name	48 h	96 h	
1	IPI00418169	ANXA2	Annexin A2	1.0795	0.8555*	Cell growth
2	IPI00553153	ATPIF1	ATPase inhibitory factor 1	1.3295*	1.2685*	Cell proliferation
3	IPI00299024	BASP1	Brain abundant, membrane attached signal protein 1	0.912	1.254*	
4	IPI00297579	CBX3	Chromobox homolog 3	1.2815	1.273*	Transcription, macromolecule biosynthetic and metabolic process
5	IPI00141318	CKAP4	Cytoskeleton-associated protein 4	0.858	0.832*	
6	IPI00011062	CPS1	Isoform 1 of Carbamoyl-phosphate synthase	1.002	0.863*	Translation
7	IPI00844578	DHX9	DEAH (Asp-Glu-Ala-His) box polypeptide 9	0.8175*	0.893	RNA splicing
8	IPI00003438	DNAJC8	DNA-J (Hsp40) homolog, subfamily C, member 8	1.268*	1.2825*	RNA splicing
9	IPI00178440	EEF1B2	Elongation factor 1-beta	1.156*	0.902	Translational elongation
10	IPI00023048	EEF1D	Eukaryotic translation elongation factor 1 delta	0.804*	1.0875	Translation, signal transduction
11	IPI00021728	EIF2S2	Eukaryotic translation initiation factor 2, subunit 2 beta	1.333*	1.1765	Translational initiation
12	IPI00290460	EIF3G	Eukaryotic translation initiation factor 3, subunit G	1.311*	1.2715	Translational initiation
13	IPI00012079	EIF4B	Eukaryotic translation initiation factor 4B	0.765*	0.9235	Cell proliferation
14	IPI00220797	ENSA	Endosulfine alpha	2.249*	1.7125	Response to extracellular stimulus
15	IPI00010951	EPPK1		0.7065*	0.872	Catabolic process
16	IPI00029631	ERH	Enhancer of rudimentary homolog	1.238*	0.868	Nucleoside metabolic process
17	IPI00009841	EWSR1	Ewing sarcoma breakpoint region 1	1.2995*	1.3885*	Transcription, RNA metabolic process
18	IPI00375441	FUBP1	Isoform 1 of far upstream element-binding protein 1	1.0765	1.116*	Transcription, RNA biosynthetic process
19	IPI00219018	GAPDH	Glyceraldehyde-3-phosphate dehydrogenase	0.8925	0.859*	Carbohydrate catabolic process
20	IPI00018278	H2AFV	Histone H2A.V	1.1445	1.3955*	Protein-DNA complex assembly
21	IPI00020956	HDGF	Hepatoma-derived growth factor	1.2445*	1.2535*	Cell proliferation
22	IPI00453473	HIST2H4B	Histone H4	1.3875*	0.965	Protein-DNA complex assembly
23	IPI00217477	HMGB3	High mobility group protein B3	1.537*	1.2635*	Regulation of immune system process
24	IPI00215965	HNRNPA1	Isoform A1-B of heterogeneous nuclear ribonucleoprotein A1	1.0265	1.129*	RNA splicing
25	IPI00028888	HNRNPD	Isoform 1 of heterogeneous nuclear ribonucleoprotein D0	1.302*	1.1335*	RNA splicing
26	IPI00479786	KHSRP	Isoform 1 of far upstream element-binding protein 2	0.978	1.171*	Transcription
27	IPI00009865	KRT10	Keratin, type I cytoskeletal 10	0.596*	0.7915	Ectoderm development, epidermis development
28	IPI00554788	KRT18	Keratin, type I cytoskeletal 18	0.8845*	1.0345	Intracellular protein transport
29	IPI00000861	LASP1	Isoform 1 of LIM and SH3 domain protein 1	1.27	0.8085*	Ion transport, cytoskeleton organization
30	IPI00219219	LGALS1	Galectin-1	0.8505	0.7385*	Apoptosis, cell death
31	IPI00006207	LRRFIP1	Isoform 2 of leucine-rich repeat flightless-interacting protein 1	1.4535*	0.994	Transcription, regulation of macromolecule metabolic process
32	IPI00219301	MARCKS	Myristoylated alanine-rich C-kinase substrate	1.1685	1.422*	Cell motility, phagocytosis, cell cycle
33	IPI00004233	MK167	Isoform long of antigen KI-67	1.2545	1.27*	Cell cycle, cell proliferation
34	IPI00019502	MYH9	Isoform 1 of myosin-9	1.0935*	1.142	Cell cycle
35	IPI00604620	NCL	Nucleolin	1.048	1.241*	Angiogenesis
36	IPI00216654	NOLC1	Isoform beta of nucleolar and coiled-body phosphoprotein 1	1.8053	1.683*	Cell cycle
37	IPI00013297	PDAP1	28 kDa heat- and acid-stable phosphoprotein	1.492*	1.13	Cell proliferation
38	IPI00299571	PDIA6	Isoform 2 of Protein disulfide-isomerase A6	0.7335*	0.858	Protein folding, cellular homeostasis
39	IPI00026154	PRKCSH	cDNA FLJ59211, highly similar to glucosidase 2 subunit beta	0.844*	1.043	Intracellular signaling cascade
40	IPI00008527	RPLP1	60S acidic ribosomal protein P1	0.644*	0.882	Translational elongation
41	IPI00008529	RPLP2	60S acidic ribosomal protein P2	1.4515*	1.0955	Translational elongation
42	IPI00013917	RPS12	40S ribosomal protein S12	0.993	0.839*	Translational elongation
43	IPI00179330	RPS27A	Ubiquitin-40S ribosomal protein S27a	1.013*	1.1595	Mitotic cell cycle, cell morphogenesis
44	IPI00026089	SF3B1	Splicing factor 3B subunit 1	1.347*	1.154	RNA splicing
45	IPI00032827	SF3B14	Pre-mRNA branch site protein p14	0.628*	0.886	RNA splicing
46	IPI00165041	TCOF1	Isoform 6 of treacle protein	0.886	1.286*	Transcription
47	IPI00414101	TOP2A	Isoform 2 of DNA topoisomerase 2-alpha	1.3335	1.603*	DNA replication, DNA metabolic process
48	IPI00221178	TPD52L2	Isoform 2 of tumor protein D54	0.985	1.223*	Cell proliferation
49	IPI00465028	TPI1	Triosephosphate isomerase isoform 2	0.9085	0.8545*	Carbohydrate biosynthetic and catabolic process
50	IPI00027107	TUFM	Elongation factor Tu, mitochondrial precursor	0.859*	0.902	Translational elongation
51	IPI00216298	TXN	Thioredoxin	1.2725*	1.1575	Cell motion, cell–cell signaling
52	IPI00022774	VCP	Transitional endoplasmic reticulum ATPase	0.9435	0.8305*	DNA replication, DNA metabolic process

* $P < 0.05$.

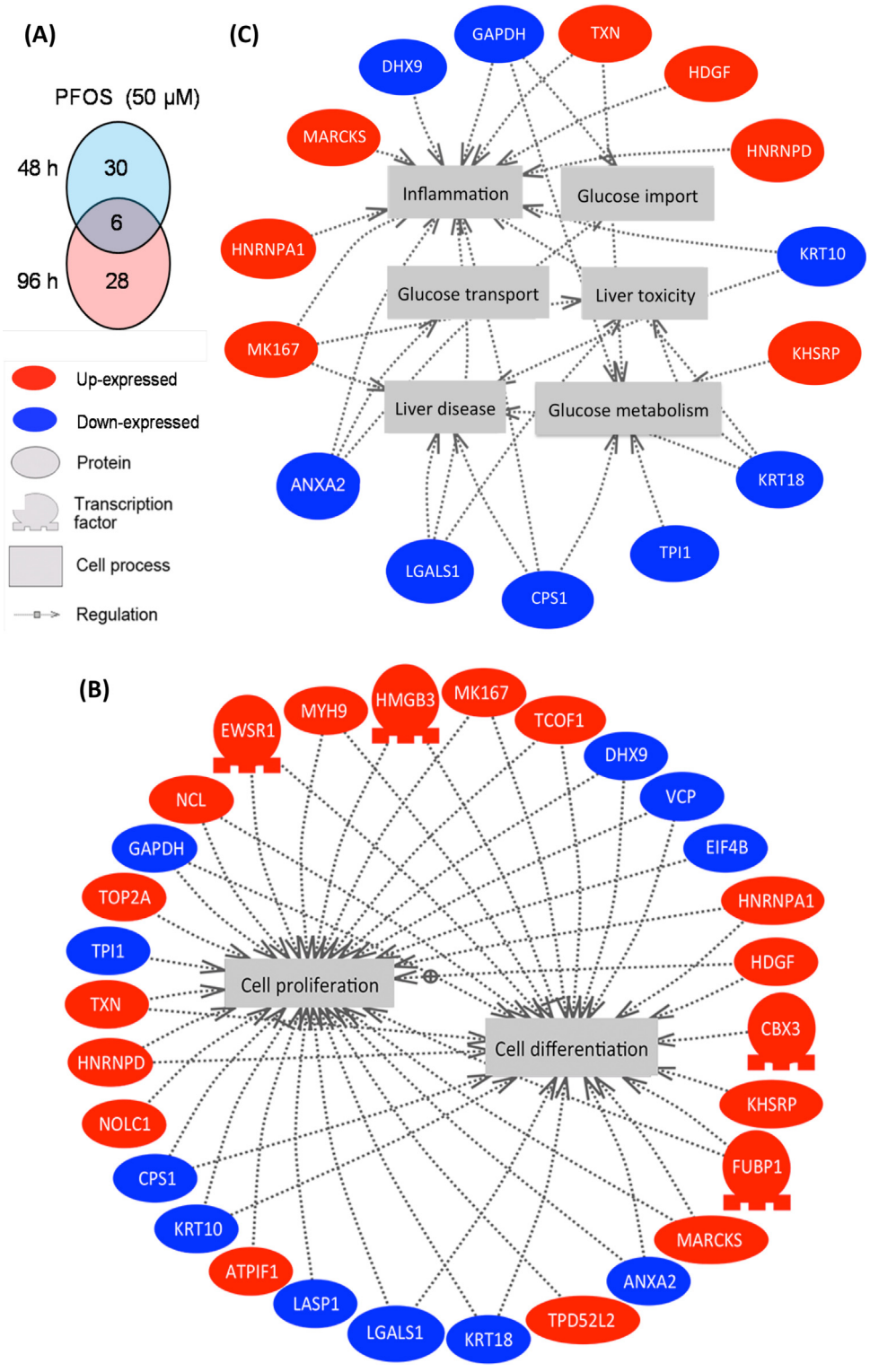

Fig. 1. Analysis of the differentially expressed proteins identified in the HL-7702 cell line treated with PFOS. Pathway analysis was performed using Pathway Studio (v 7.0) software. (A) Number of differentially expressed proteins in HL-7702 from the solvent control and groups exposed to PFOS for 48 h and 96 h. (B) Network of cell proliferation and differentiation processes. (C) Network of liver disease.

to analyze the protein samples from the HL-7702 cells of the control and 50 μM PFOS-treated group following 48 h and 96 h exposure. Quantitative analysis and identification of LC-MS/MS spectra revealed a total of 170,743 and 171,103 mass spectra in the two replicates, respectively. Searching Mascot 2.3.02 identified a total of 2,025 and 2,048 proteins comprised of 6,571 and 6,656 unique peptides in the two replicates, respectively, in which 5,024 peptides were identical between the replicates. The proteins that were both up-regulated or both down-regulated significantly ($P < 0.05$) in the two replicates were chosen for further analysis. After filtering, a total of 52 proteins were significantly differentially expressed (Table 1), including 30 (19 up-regulated and 11 down-regulated)

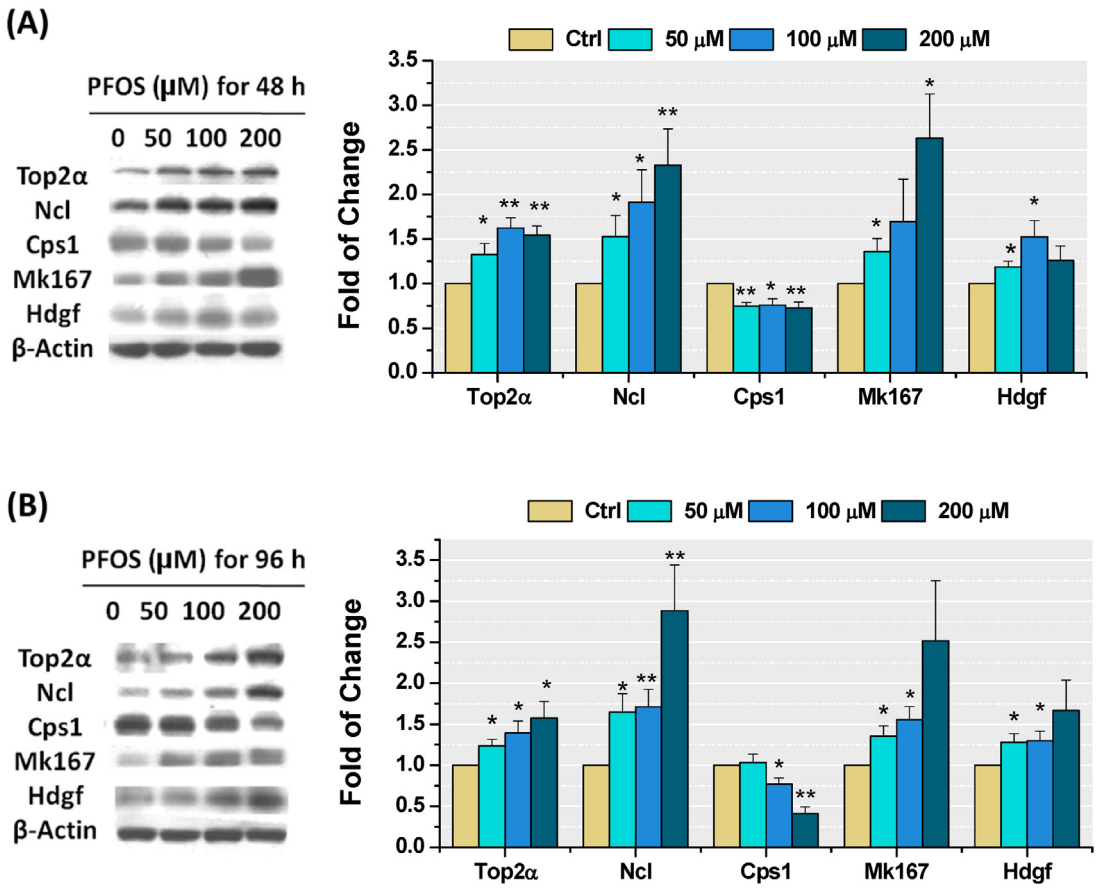

Fig. 2. Western blot verification of proteins identified in the iTRAQ results following PFOS exposure for 48 h (A) and 96 h (B). The left panel shows representative blots from three experiments. The right panel shows the mean levels of protein bands compared with the control, values indicate mean ± SE ($n = 3$) (*: $P < 0.05$, **: $P < 0.01$).

and 28 (19 up-regulated and 9 down-regulated) proteins in the 48 h and 96 h PFOS (50 μM)-treated groups compared with the control, respectively (Fig. 1A).

To gain a better understanding of the identified proteins, Gene Ontology (GO) annotation was done by searching the GO web site (http://www.geneontology.org). Gene Ontology data, including molecular functions, cellular components and biological processes of the differential expressed proteins, were analyzed and sorted. The most significantly overrepresented cellular functions were related to binding and catalytic activity. The most significantly overrepresented biological processes were cellular and metabolic processes.

Detailed analyses of the interaction relationships among these proteins were performed using Pathway Studio software via the ResNet database. From the total of 52 proteins, 29 were associated with cell proliferation (27 proteins) and cell differentiation (22 proteins) directly or indirectly (Fig. 1B) and 15 were related to inflammation, glucose import, transport and metabolism, liver toxicity, and liver disease (Fig. 1C).

Top2α, Ncl, Cps1, Mk167 (Ki67), and Hdgf associated with cell proliferation were chosen for verification using western blot analysis (Fig. 2). All protein levels in the 50 μM or higher dose groups supported the above findings. This confirmed the initial iTRAQ data, indicating that the iTRAQ results were credible.

3.2. Effect of PFOS on cell proliferation

The MTT results (Fig. 3A) showed that after 48 h and 96 h, the HL-7702 cells were stimulated to proliferate at low PFOS doses (until 200 μM). The highest stimulatory effects appeared at 100 μM after 48 h and at 50 μM after 96 h, with maximal cell viabilities of 158.5% and 155.0%, respectively. Similarly, cell numbers increased significantly in the 100 μM and 200 μM PFOS exposure groups after 48 h but the largest increase appeared in the 200 μM group. At 96 h, the changes in cell number had the same tendency as that of the MTT results (Fig. 3B).

3.3. Effect of PFOS on the cell cycle

Flow cytometry showed that treatment with PFOS did not cause apoptosis but did change the cell cycle distribution of HL-7702 after 48 h and 96 h (Table 2). The G0/G1 phase percentage was reduced

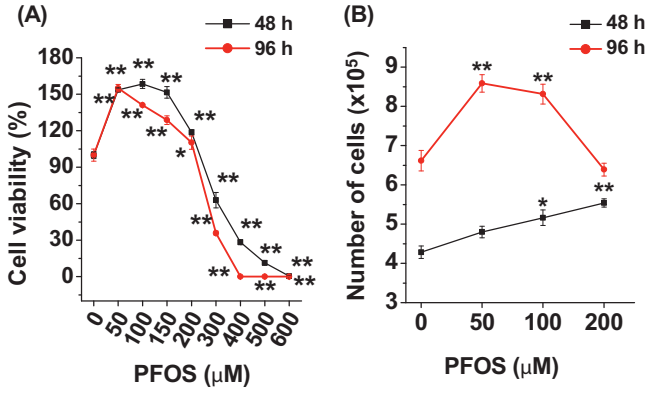

Fig. 3. Dose-response between PFOS concentration and cell viability (A) and cell number (B) of HL-7702 following 48 h and 96 h exposure (*: $P < 0.05$, **: $P < 0.01$).

Table 2
Effects of PFOS on cell cycle distribution.

PFOS (μM)		G0/G1 phase		S phase %	G2/M phase		S + G2/M %	Apoptosis %
		DNA content	%		DNA content	%		
48 h	0	52.79 ± 0.31	81.52 ± 0.20	13.29 ± 0.23	103.58 ± 0.74	5.20 ± 0.05	18.49 ± 0.20	0.54 ± 0.21
	50	52.71 ± 0.48	77.86 ± 1.07*	15.74 ± 0.25**	103.19 ± 0.81	5.40 ± 0.14	21.14 ± 0.15**	0.44 ± 0.24
	100	51.07 ± 0.10**	77.70 ± 0.12**	16.57 ± 0.11**	100.13 ± 0.14*	5.73 ± 0.20*	22.30 ± 0.12**	0.55 ± 0.40
	200	50.26 ± 0.05**	76.75 ± 0.18**	18.59 ± 0.08**	98.56 ± 0.14**	4.66 ± 0.19*	23.25 ± 0.18**	0.32 ± 0.10
96 h	0	51.20 ± 0.67	76.82 ± 0.33	16.76 ± 0.37	100.02 ± 1.21	6.43 ± 0.14	23.18 ± 0.33	0.12 ± 0.06
	50	52.36 ± 0.02	72.81 ± 0.22**	21.03 ± 0.12**	102.57 ± 0.22	6.16 ± 0.21	27.19 ± 0.22**	0.93 ± 0.75
	100	52.19 ± 0.63	73.16 ± 0.22**	20.94 ± 0.44**	102.22 ± 1.01	5.89 ± 0.23	26.84 ± 0.22**	0.15 ± 0.01
	200	49.91 ± 0.38	75.26 ± 0.62	19.88 ± 0.62*	98.92 ± 0.50	4.85 ± 0.24**	24.74 ± 0.62	0.16 ± 0.05

$n = 3$.
* $P < 0.05$; ** $P < 0.01$.

while the S phase percentage was induced in all dose groups, except that no change occurred in the G0/G1 phase in the 200 μM group after 96 h. The G2/M percentage increased in the 100 μM group after 48 h, but declined in the 200 μM group after 48 h and 96 h exposure.

3.4. Effect of PFOS on the protein levels involved in the cell cycle

Proteins like cyclins, which regulate the cell cycle, were disrupted or induced by PFOS (Fig. 4). After PFOS treatment for 48 h, the levels of Cyclin D1, which controls G1 progression, and its partner cyclin-dependent kinase 6 (Cdk6) were induced in a dose-dependent manner. At 50 μM and 100 μM, the expressions of Cyclin E2 and Cyclin A2, which control G1 progression, DNA synthesis and G1/S and G2/M transitions, were increased compared with those of the control group. Their partner cyclin-dependent kinase 2 (Cdk2) was also induced by PFOS in a dose-dependent manner. Cyclin B1, which plays a key role in G2 and M progression, was up-regulated after 50 μM and 100 μM PFOS exposure. The key phosphorylations of checkpoint proteins p-Chk1 (S345) and p-Chk2 (T68) were down-regulated and up-regulated, respectively, in the higher-dose groups. Levels of p53 were unchanged after PFOS exposure, but c-Myc was up-regulated in the 200 μM group and its down-stream protein p21 waf1/cip1 was significantly down-regulated in the higher-dose groups. In addition, p-Wee1 (S642), Myt1 and p-Cdc2 (Y15) were up-regulated in several exposure groups.

After PFOS exposure for 96 h, the expressions of the above proteins exhibited some different patterns from those exhibited after 48 h exposure. There was no significant differential expression of Cyclin B1 in the PFOS groups compared with the control. Cyclin D1 was up-regulated in the 50 μM and 100 μM groups and Cdk6 increased at 50 μM and 200 μM. Cyclin E2 was up-regulated in the 50 μM group, but down-regulated in the 200 μM group. Cyclin A2 and its catalytic partner Cdk2 were induced by PFOS in the 50 μM and 100 μM groups. Checkpoint proteins had similar trends after 48 h exposure. Furthermore, p53 decreased in the 200 μM group, c-Myc was up-regulated in the 200 μM group and p21 waf1/cip1 was reduced in a dose-dependent manner. The expressions of p-Wee1 (S642) and p-Cdc2 (Y15) rose in the PFOS-exposed groups, while Myt1 exhibited no differential expression. A possible schematic model of how PFOS promotes cell cycle progression and stimulates cell proliferation is given in Fig. 5.

4. Discussion

Our iTRAQ analysis showed that 27 out of 52 differentially expressed proteins were associated with cell proliferation. Among these proteins, the widely used proliferation markers Mk167 (Ki67) and Top2α [23,24] and the nuclear targeted mitogen Hdgf [25,26] were all induced by PFOS exposure, as determined by iTRAQ assay and confirmed by western blot assay. These data suggest that PFOS probably stimulated HL-7702 proliferation under the experimental conditions. However, previous proteomic analyses [27,28], which identified differentially expressed proteins responsive to PFOS exposure, suggested PFOS induced HL-7702 cell apoptosis via p53 and c-Myc. In our study, PFOS stimulated proliferation and did not induce significant apoptosis (under 1%). The present research provides a different view on the effect of PFOS on HL-7702.

Our MTT and cell counting results provided clear evidence that exposure to PFOS at doses lower than 200 μM obviously stimulated cell proliferation, in accordance with previous research [29]. The cell cycle distribution data showed that the reduced G0/G1 phase percentage and increased S phase percentage resulted from PFOS exposure for 48 h and 96 h, indicating that PFOS drove more resting HL-7702 cells into the cell cycle from the quiescence stage (G0). Furthermore, the (S + G2/M)% accurately corresponded to the alteration in cell number. In particular, the largest (S + G2/M)% (indicating the greatest proliferation ability) was observed in the 200 μM group at 48 h, which coincided with the largest increase in cell number. This differed from the MTT results, in which maximum cell viability appeared at 100 μM but not 200 μM. This difference might be related to the fact that the MTT assay determined the activity of the NAD(P)H-dependent cellular oxidoreductase enzyme as an indirect parameter of cell viability. At 96 h, the (S + G2/M)% of the 200 μM group was no longer larger than that of the control group, suggesting that the cell number in the 200 μM group did not increase much. It was supposed that 200 μM PFOS exposure for 96 h induced an inhibitory effect but no longer an stimulatory effect.

Resting cells have to be stimulated by growth factors to enter the cell cycle, beginning with the G1 phase. The induction of Hdgf by PFOS might contribute to this progression. Following growth factor stimulation, a variety of signaling pathways transmit information to the nucleus and activate the transcription of Cyclin D1, which is essential for G1/S progression. Subsequently, Cyclin D1 starts to accumulate and assemble with its catalytic partners Cdk4 and Cdk6 [30]. The amount of Cyclin D1 fluctuates at a high level throughout the whole cell cycle, which means that daughter cells are able to enter the next cell cycle once they complete mitosis. If the level of Cyclin D1 falls, daughter cells will exit the cell cycle and enter the G0 state [31]. Cyclin D1 acts on retinoblastoma protein (Rb) to remove its inhibitory effect on E2F, which then transactivates Cyclin E and Cyclin A such that they can act together to initiate DNA synthesis. Cyclin E pairs up with Cdk2 to form Cyclin E/Cdk2 complexes, which contribute to G1 progression and the onset of DNA synthesis [32]. Maximum amounts of Cyclin E and Cyclin E/Cdk2 are reached in the late G1 and early S phases [33]. After the level of Cyclin E falls, its role in DNA synthesis is then taken over by Cyclin A. Cyclin A can also assemble with Cdk2 to form Cyclin A/Cdk2 complexes, and provide a link between the early events in G1 and the final events that occur during the G2/M phase [32]. Once DNA synthesis is complete, cells exit the S phase and enter the G2 phase to begin

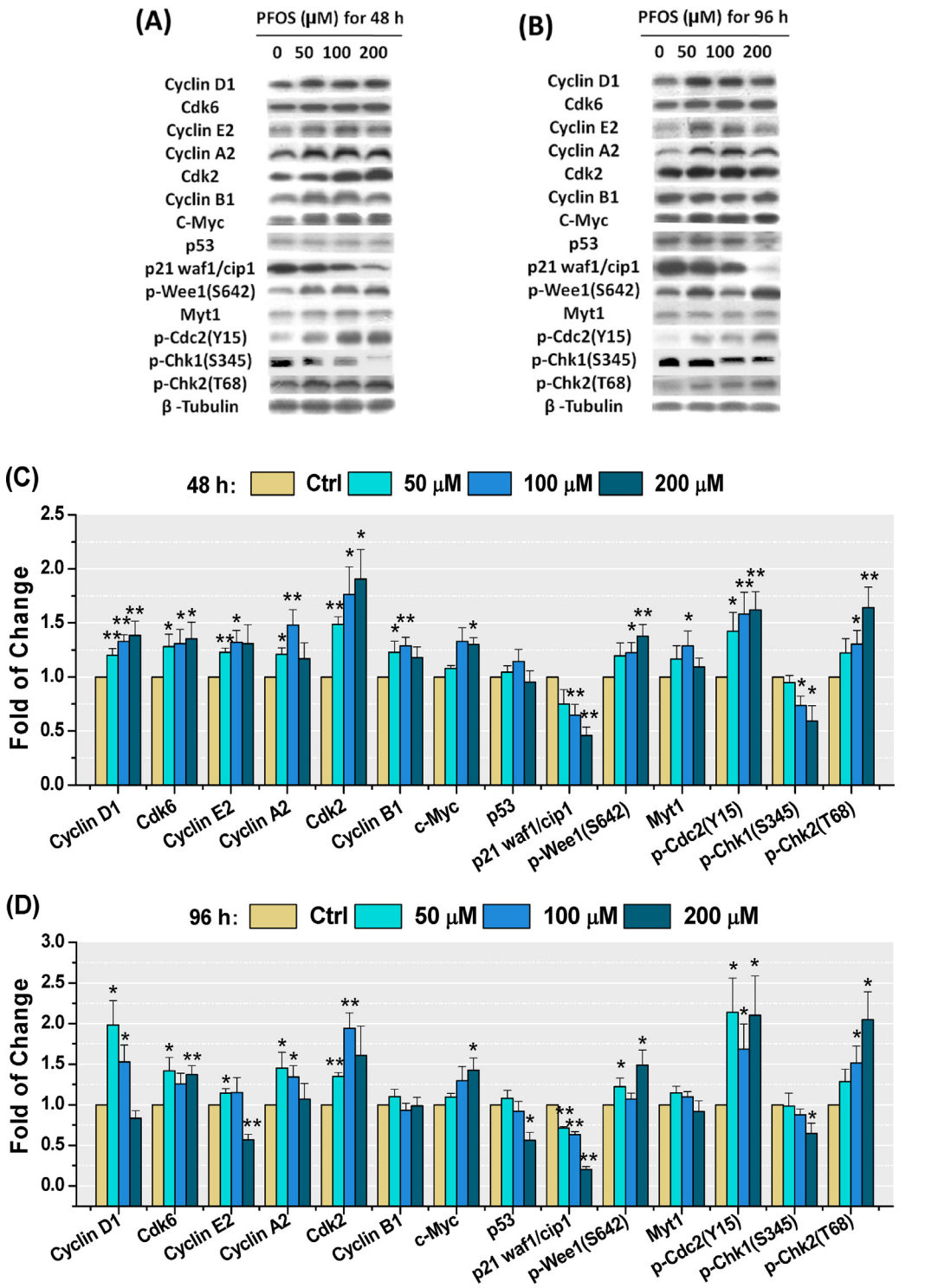

Fig. 4. Western blot analysis of the expression of cell cycle-related proteins after PFOS treatment on HL-7702 cells for 48 h (A/C) and 96 h (B/D) A and B: representative blots from three experiments; C and D: relative fold change of protein band densities, values indicate mean ± SE ($n = 3$) (*: $P < 0.05$,**: $P < 0.01$).

mitosis. The Cyclin B1/Cdk1 complex plays a key role in G2/M transition and M phase progression. The entry into the M phase depends on the activation of the Cyclin B1/Cdk1 complex, whose activity is inhibited by the phosphorylation of Cdk1 on Tyr15 and Thr14 sites by Wee1 and Myt1 until inhibitory phosphates are removed by Cdc25B/C and the active complex then enters the nucleus to initiate mitosis [34]. In our study, the increases in Cyclin D1 and its partner Cdk6 induced by PFOS exposure significantly corresponded with a reduced G0/G1 phase percentage, indicating that more cells were driven by PFOS into the cell cycle from the G0 phase. The up-regulations of Cyclin E2, Cyclin A2 and Cdk2 following 48 h and 96 h PFOS exposure were associated with an increased S phase percentage. The induced Cyclin B1, which promotes G2/M transition, might have contributed to the increased G2/M phase percentage (as seen in the 50 and 100 μM groups at 48 h).

We also investigated protein levels of several other regulators. The levels of activated phosphorylation of checkpoint proteins, p-Chk1 (S345) and p-Chk2 (T68), were down-regulated

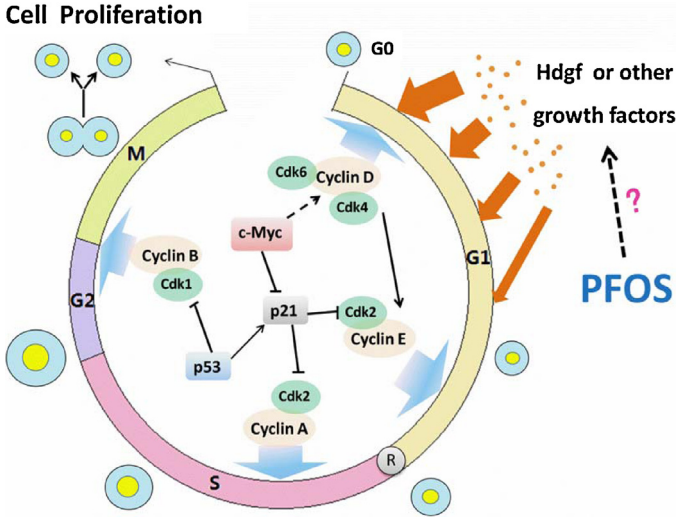

Fig. 5. Possible schematic model of how PFOS promotes cell cycle progression and stimulates cell proliferation. PFOS enhances the expression of growth factor Hdgf and up-regulates cyclins/cdks, especially Cyclin D1, to drive cells into the cell cycle from the quiescence stage (G0) and promote cell cycle progression.

and up-regulated in the higher-dose groups after 48 h and 96 h, respectively. The mechanism of this situation remains unclear, although the effects of these two checkpoint proteins may offset each other, so their down-stream protein p53 did not change significantly (except 200 μM at 96 h) and the expressions of cyclins and cdks were not affected. The decrease in p21 waf1/cip1, which acts as an inhibitor of Cdk2 complexes and is a down-stream protein of the p53 pathway, might have resulted from the up-regulation of c-Myc, which can induce cell proliferation in established cell lines [35,36]. It is worth noting that the expressions of p-Wee1 (S642) and p-Cdc2 (Y15) increased in the PFOS-treated groups. Wee1 holds the molecular switch for G2/M transition by phosphorylating Cdc2 (Cdk1). S642 phosphorylation of Wee1 promotes the nuclear-to-cytoplasmic translocation of Wee1 without affecting its kinase activity to promote G2/M cell cycle progression [37]. The inactivated phosphorylation of Cdc2 at Y15, which keeps the Cyclin B1/Cdc2 (Cdk1) complex from entering the nucleus, might be due to the increased cytoplasmic Wee1 or increased total Cdc2 protein amount, and therefore it is difficult to determine whether the increase in p-Cdc2 (Y15) affected cell cycle progression positively or negatively. In addition, the 200 μM PFOS dose affected the differential expression of the above proteins (p-Chk1 (S345), p-Chk2 (T68), p53, p21 waf1/cip1, c-Myc, p-Wee1 (S642), Myt1 and p-Cdc2 (Y15)) at 48 h and 96 h. For instance, after 200 μM PFOS exposure, the expressions of Cyclin D1 and Cdk2 increased at 48 h but did not change at 96 h; the level of Cyclin E2 did not change at 48 h but decreased at 96 h. These results might explain why the G0/G1 phase percentage decreased at 48 h but did not change at 96 h. We supposed that 200 μM exposure for 96 h might cause S phase arrest, unlike the same exposure for 48 h, which might promote S phase progression.

In addition, we speculated that ligand length sensitive G-protein coupled receptors (GPCRs), which are activated by short- and long-chain free fatty acids, might be involved in the process by which PFOS affected cell proliferation through the ERK, PI3K-Akt and MAPK pathways [38,39].

In conclusion, our present study provides new insight on PFOS-induced hepatotoxicity. Using a iTRAQ labeling quantitative proteomic technique, we found that most differentially expressed proteins were associated with cell proliferation. Furthermore, low doses of PFOS (under 200 μM) enhanced the expression of growth factor Hdgf and proliferation biomarkers Mk167 (Ki67) and Top2α. The up-regulation in the expression of cyclins/cdks (especially Cyclin D1) following PFOS exposure may have driven cells into the cell cycle from the quiescence stage (G0) and altered other regulating proteins to promote cell cycle progression. To our knowledge, this is the first study to investigate the mechanism of how PFOS affects liver cell proliferation, which will help provide novel insight into the molecular mechanisms involved in PFOS-induced hepatocellular hypertrophy.

Acknowledgements

This work was supported by the Strategic Priority Research Program of the Chinese Academy of Sciences (XDB14040202), the National High-Tech R&D Plan (863 Program: 2013AA065203) and the National Natural Science Foundation of China (grants No. 31320103915 and 21377128).

References

[1] E. Kissa, Fluorinated Surfactants and Repellents, Marcel Dekker, New York, 2001.
[2] B. Raj Shivakoti, S. Tanaka, S. Fujii, N.P. Hong Lien, M. Nozoe, C. Kunacheva, R. Okamoto, S.T. Seneviratne, H. Tanaka, Perfluorinated compounds (pfcs) in yodo river system, japan, Water Sci. Technol. 63 (2011) 115–123.
[3] K. Harada, S. Nakanishi, K. Sasaki, K. Furuyama, S. Nakayama, N. Saito, K. Yamakawa, A. Koizumi, Particle size distribution and respiratory deposition estimates of airborne perfluorooctanoate and perfluorooctanesulfonate in kyoto area, japan, Bull. Environ. Contam. Toxicol. 76 (2006) 306–310.
[4] C.P. Higgins, J.A. Field, C.S. Criddle, R.G. Luthy, Quantitative determination of perfluorochemicals in sediments and domestic sludge, Environ. Sci. Technol. 39 (2005) 3946–3956.
[5] G.T. Tomy, W. Budakowski, T. Halldorson, P.A. Helm, G.A. Stern, K. Friesen, K. Pepper, S.A. Tittlemier, A.T. Fisk, Fluorinated organic compounds in an eastern arctic marine food web, Environ. Sci. Technol. 38 (2004) 6475–6481.
[6] A.M. Calafat, Z. Kuklenyik, S.P. Caudill, J.A. Reidy, L.L. Needham, Perfluorochemicals in pooled serum samples from united states residents in 2001 and 2002, Environ. Sci. Technol. 40 (2006) 2128–2134.
[7] B.J. Apelberg, F.R. Witter, J.B. Herbstman, A.M. Calafat, R.U. Halden, L.L. Needham, L.R. Goldman, Cord serum concentrations of perfluorooctane sulfonate (pfos) and perfluorooctanoate (pfoa) in relation to weight and size at birth, Environ. Health Perspect. 115 (2007) 1670–1676.
[8] K.S. Guruge, S. Taniyasu, N. Yamashita, S. Wijeratna, K.M. Mohotti, H.R. Seneviratne, K. Kannan, N. Yamanaka, S. Miyazaki, Perfluorinated organic compounds in human blood serum and seminal plasma: A study of urban and rural tea worker populations in sri lanka, J. Environ. Monit. 7 (2005) 371–377.
[9] C.R. Stein, M.S. Wolff, A.M. Calafat, K. Kato, S.M. Engel, Comparison of polyfluoroalkyl compound concentrations in maternal serum and amniotic fluid: A pilot study, Reprod. Toxicol. 34 (2012) 312–316.
[10] G.W. Olsen, J.M. Burris, D.J. Ehresman, J.W. Froehlich, A.M. Seacat, J.L. Butenhoff, L.R. Zobel, Half-life of serum elimination of perfluorooctanesulfonate,perfluorohexanesulfonate, and perfluorooctanoate in retired fluorochemical production workers, Environ, Health Perspect. 115 (2007) 1298–1305.
[11] K. Steenland, S. Tinker, S. Frisbee, A. Ducatman, V. Vaccarino, Association of perfluorooctanoic acid and perfluorooctane sulfonate with serum lipids among adults living near a chemical plant, Am. J. Epidemiol. 170 (2009) 1268–1278.
[12] S.J. Frisbee, A. Shankar, S.S. Knox, K. Steenland, D.A. Savitz, T. Fletcher, A.M. Ducatman, Perfluorooctanoic acid, perfluorooctanesulfonate, and serum lipids in children and adolescents: Results from the c8 health project, Arch. Pediatr. Adolesc. Med. 164 (2010) 860–869.
[13] J.W. Nelson, E.E. Hatch, T.F. Webster, Exposure to polyfluoroalkyl chemicals and cholesterol body weight, and insulin resistance in the general U.S. population, Environ. Health Perspect. 118 (2010) 197–202.
[14] K. Steenland, S. Tinker, A. Shankar, A. Ducatman, Association of perfluorooctanoic acid (pfoa) and perfluorooctane sulfonate (pfos) with uric acid among adults with elevated community exposure to pfoa, Environ. Health Perspect. 118 (2010) 229–233.
[15] U.N. Joensen, R. Bossi, H. Leffers, A.A. Jensen, N.E. Skakkebaek, N. Jorgensen, Do perfluoroalkyl compounds impair human semen quality? Environ. Health Perspect. 117 (2009) 923–927.
[16] A. Hagenaars, D. Knapen, I.J. Meyer, K. van der Ven, P. Hoff, W. De Coen, Toxicity evaluation of perfluorooctane sulfonate (pfos) in the liver of common carp (cyprinus carpio), Aquat. Toxicol. 88 (2008) 155–163.
[17] M.B. Rosen, J.R. Schmid, J.C. Corton, R.D. Zehr, K.P. Das, B.D. Abbott, C. Lau, Gene expression profiling in wild-type and pparalpha-null mice exposed to perfluorooctane sulfonate reveals pparalpha-independent effects, PPAR Res 2010 (2010).

[18] L.B. Biegel, M.E. Hurtt, S.R. Frame, J.C. O'Connor, J.C. Cook, Mechanisms of extrahepatic tumor induction by peroxisome proliferators in male cd rats, Toxicol. Sci. 60 (2001) 44–55.
[19] C.R. Elcombe, B.M. Elcombe, J.R. Foster, S.C. Chang, D.J. Ehresman, J.L. Butenhoff, Hepatocellular hypertrophy and cell proliferation in sprague-dawley rats from dietary exposure to potassium perfluorooctanesulfonate results from increased expression of xenosensor nuclear receptors pparalpha and car/pxr, Toxicology 293 (2012) 16–29.
[20] M.B. Rosen, K.P. Das, C.R. Wood, C.J. Wolf, B.D. Abbott, C. Lau, Evaluation of perfluoroalkyl acid activity using primary mouse and human hepatocytes, Toxicology 308 (2013) 129–137.
[21] M.L. Takacs, B.D. Abbott, Activation of mouse and human peroxisome proliferator-activated receptors (alpha beta/delta, gamma) by perfluorooctanoic acid and perfluorooctane sulfonate, Toxicol. Sci. 95 (2007) 108–117.
[22] Z. Shi, H. Zhang, L. Ding, Y. Feng, J. Wang, J. Dai, Proteomic analysis for testis of rats chronically exposed to perfluorododecanoic acid, Toxicol. Lett. 192 (2010) 179–188.
[23] K. Milde-Langosch, T. Karn, V. Muller, I. Witzel, A. Rody, M. Schmidt, R.M. Wirtz, Validity of the proliferation markers ki67 top2a, and racgap1 in molecular subgroups of breast cancer, Breast Cancer Res. Treat. 137 (2013) 57–67.
[24] L.T. Li, G. Jiang, Q. Chen, J.N. Zheng, Ki67 is a promising molecular target in the diagnosis of cancer (review), Mol. Med. Rep. 11 (2015) 1566–1572.
[25] Y. Kishima, H. Yamamoto, Y. Izumoto, K. Yoshida, H. Enomoto, M. Yamamoto, T. Kuroda, H. Ito, K. Yoshizaki, H. Nakamura, Hepatoma-derived growth factor stimulates cell growth after translocation to the nucleus by nuclear localization signals, J. Biol. Chem. 277 (2002) 10315–10322.
[26] A.D. Everett, J. Bushweller, Hepatoma derived growth factor is a nuclear targeted mitogen, Curr. Drug Targets 4 (2003) 367–371.
[27] Q. Huang, J. Zhang, S. Peng, M. Du, S. Ow, H. Pu, C. Pan, H. Shen, Proteomic analysis of perfluorooctane sulfonate-induced apoptosis in human hepatic cells using the itraq technique, J. Appl. Toxicol. 34 (2014) 1342–1351.
[28] F. Tan, Y. Jin, W. Liu, X. Quan, J. Chen, Z. Liang, Global liver proteome analysis using itraq labeling quantitative proteomic technology to reveal biomarkers in mice exposed to perfluorooctane sulfonate (pfos), Environ. Sci. Technol. 46 (2012) 12170–12177.
[29] J. Hu, J. Li, J. Wang, A. Zhang, J. Dai, Synergistic effects of perfluoroalkyl acids mixtures with j-shaped concentration-responses on viability of a human liver cell line, Chemosphere 96 (2014) 81–88.
[30] M.V. Blagosklonny, A.B. Pardee, The restriction point of the cell cycle, Cell Cycle 1 (2002) 103–110.
[31] Y. Guo, J. Harwalkar, D.W. Stacey, M. Hitomi, Destabilization of cyclin d1 message plays a critical role in cell cycle exit upon mitogen withdrawal, Oncogene 24 (2005) 1032–1042.
[32] E. Lees, B. Faha, V. Dulic, S.I. Reed, E. Harlow, Cyclin e/cdk2 and cyclin a/cdk2 kinases associate with p107 and e2f in a temporally distinct manner, Genes Dev. 6 (1992) 1874–1885.
[33] V. Dulic, E. Lees, S.I. Reed, Association of human cyclin e with a periodic g1-s phase protein kinase, Science 257 (1992) 1958–1961.
[34] J.P. Chow, R.Y. Poon, The cdk1 inhibitory kinase myt1 in DNA damage checkpoint recovery, Oncogene 32 (2013) 4778–4788.
[35] A.J. Obaya, M.K. Mateyak, J.M. Sedivy, Mysterious liaisons: The relationship between c-myc and the cell cycle, Oncogene 18 (1999) 2934–2941.
[36] T. Hunter, Oncoprotein networks, Cell 88 (1997) 333–346.
[37] K. Katayama, N. Fujita, T. Tsuruo, Akt/protein kinase b-dependent phosphorylation and inactivation of wee1hu promote cell cycle progression at g2/m transition, Mol. Cell. Biol. 25 (2005) 5725–5737.
[38] S. Talukdar, J.M. Olefsky, O. Osborn, Targeting gpr120 and other fatty acid-sensing gpcrs ameliorates insulin resistance and inflammatory diseases, Trends Pharmacol. Sci. 32 (2011) 543–550.
[39] M.A. Vinolo, S.M. Hirabara, R. Curi, G-protein-coupled receptors as fat sensors, Curr. Opin. Clin. Nutr. Metab. Care 15 (2012) 112–116.